Supplementary Information

# A 'turn-on' Fluorescent Probe for Lysosomal Phosphatase: A Comparative Study for Labeling of Cancer Cells

Arup Podder[a], Sudipta Senapati[b], Pralay Maiti[b], Devaraj Kamalraj[c], Syed S Jaffer[c], Sabina Khatun[a], Sankarprasad Bhuniya[a,d,*],

[a]AmritaCentre for Industrial Research &Innovation, Amrita School of Engineering, Coimbatore, Amrita VishwaVidyapeetham, India 641112.

[b] School of Materials Science and Technology, Indian Institute of Technology (BHU), Vanarasi, India 221-005.

[c]Department of Chemistry, Coimbatore Institute of Technology, Coimbatore, Tamilnadu. India 641 014.

[d]Department of Chemical Engineering & Materials Science, Amrita School of Engineering, Coimbatore, Amrita VishwaVidyapeetham, India 641112.

[*] To whom correspondence should be addressed.

E-mail: b_sankarprasad@cb.amrita.edu (S. Bhuniya)

**Reaction Scheme:**

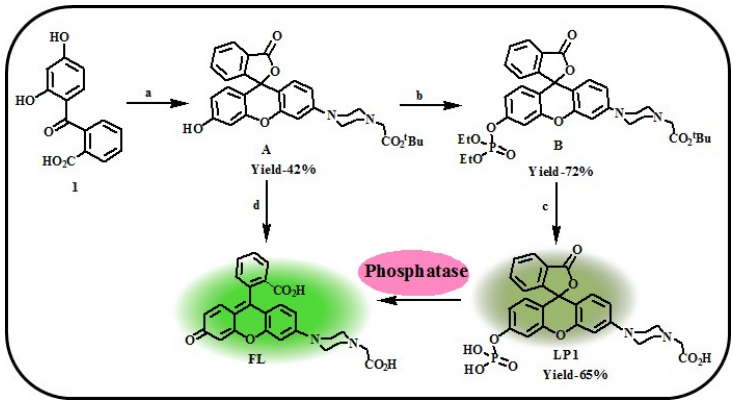


**a**: 1-(3-hydroxy phenyl)-piperazine , TFA, 95°C, 3h.then, $BrCH_2CO_2{}^tBu$, $K_2CO_3$, ACN, 85°C, 12h. **b**: $PO(OEt)_2Cl$, DIPEA, $CH_3CN$ , rt, 12h. **c**: TMSI, DCM , rt ,1h. **d**: TFA, DCM ,rt ,2h.

*General information of materials for synthesis*

1-(3-hydroxy phenyl)-piperazine (Aldrich), tert-butyl bromoacetate (Alfa-aesar), HI (Aldrich), $K_2CO_3$ (Rankem), acetonitrile (Avra), DIPEA (HIMEDIA), iodotrimethylsilane (Avra), diethylchlorophosphate (Alfa-Aesar), DMAP (HIMEDIA), trifluroacetic acid (Avra), DCM (Loba chem. India), ALP product code 12151(0148190) ex. Calf Intestine Mucosa (activity-3.43 units/mg) and ACP from wheat Germ (TCI) were purchased commercially and used without further purification. Flash column chromatography was performed using silica gel (100-200 mesh) and analytical thin layer chromatography was performed using silica gel 60 (pre coated sheets with 0.25 mm thickness). Mass spectra were recorded on anionSpecHiResESI mass spectrometer. NMR spectra were collected on a 400MHz spectrometer (Bruker, Germany).

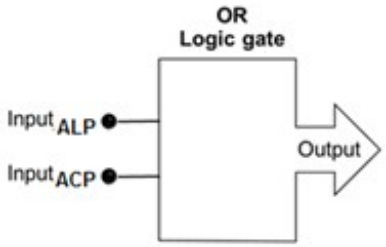


| pH-4.5 | Input ALP $\lambda_{abs}$ 490 nm at pH 4.5 | Input ACP $\lambda_{abs}$ 490 nm at pH 4.5 | Output $\lambda_{em}$ 532 nm at pH 4.5 |
|---|---|---|---|
| LP1 | 0 | 0 | 0 |
| LP1 | 1 | 0 | 1 |
| LP1 | 0 | 1 | 1 |
| LP1 | 1 | 1 | 1 |

**Table S1.** OR logic operation based on input (ALP/ACP) at pH 4.5.

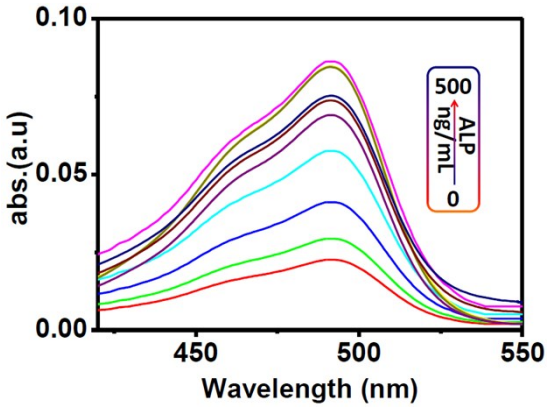


**Fig. S1.** UV study of **LP1** (10 μM) with (0-500 ng/mL) ALP at pH-4.5 in HEPES buffer solution (0.01M). All the data were acquired 60 min after addition of ALP at 37 °C.

*The Linear Range and Detection Limit*

The fluorescence titration was used to calculate the detection limit. The fluorescence emission spectrum of probe **LP1** ($2.0\times10^{-6}$ M) was measured ten times and the standard deviation of blank measurement was achieved. The fluorescence intensity at 532 nm was plotted as a concentration of ALP. The detection limit was calculated by using following equation.

*Detection Limit 3σ/k*

Where σ is the standard deviation of blank measurement, k is the slope between the fluorescence intensity versus ALP concentration.

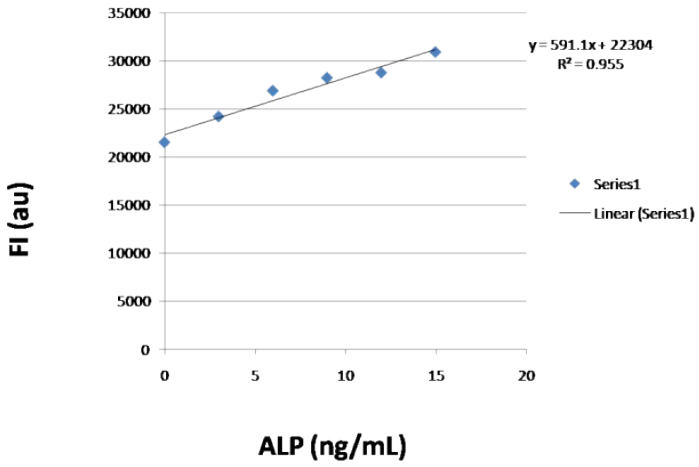


**Fig. S2.** The changes in the fluorescence intensity of **LP1** (2.0 μM) at 532 nm against varied concentrations of ALP from 0 to 20 ng/mL in HEPES buffer (0.01 M, pH 4.5) with the slit width 5/5 nm.

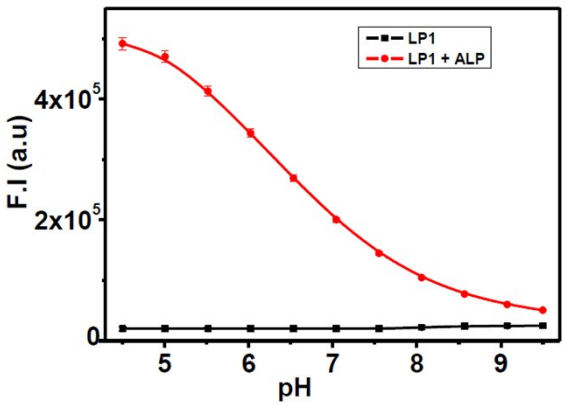


**Fig. S3.** Comparative Fluorescence study of **LP1** (10 µM ) at various pH range (4.5 - 9.5) in HEPES buffer solution (0.01M) without and with (500 ng/mL) ALP at-37 °C. Excitation at $\lambda_{ex}$ 490 nm and emmission at $\lambda_{em}$ 532 nm respectively. Excitation and emission slit widths both set at 5 nm.

| **Quantum Yield(Φ)** | **LP1(10µM) +500ng/mL ALP** | **LP1 (10µM)** |
|---|---|---|
| pH-8.5 | Φ=0.0487 | Φ=0.0201 |
| pH-4.5 | Φ=0.6126 | Φ=0.0293 |

**Fig. S4.** Quantum Yield(Φ) of **LP1**.

*pKa of probe* **LP1** with **ALP**

The pKa values for **LP1** with ALP (500 ng/mL) with a maximum excitation at 490 nm was estimated from the changes in the fluorescence intensity with various pH (4.5-9.5) values by using the relationship, $\log[(I_{max}-I)(I-I_{min})] = pH - pKa$, where $I_{max}$, $I_{min}$ and I are the maximum,

minimum and observed fluorescence intensity at a given pH, respectively. The pKa values (y-intercept) for excitation 490 nm, emission at 532 nm (pKa =6.62±0.04) were derived from the plot of pH vs log[($I_{max}$-I)(I-$I_{min}$)]. All the data were acquired 30 min after addition of ALP at 37°C.

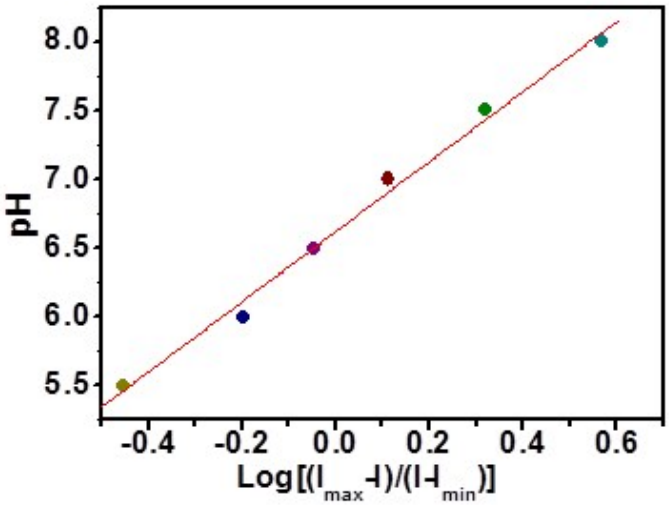


Linear Regression for Data1_A:
Y = A + B * X

| Parameter | Value | Error | |
|---|---|---|---|
| A | 6.62141 | 0.03743 | |
| B | 2.54661 | 0.11079 | |
| R | SD N | P | |
| 0.99624 | 0.09065 | 6 | <0.0001 |

**Fig. S5.** Plot of pH vs log[($I_{max}$-I)(I-$I_{min}$)], where I is the observed fluorescence intensity of **LP1** with ALP (500 ng/mL) at 532 nm upon excitation at 490 nm. The y-intercept is the pKa value (6.62141±0.03743) of equilibrium between the **LP1** and the resonance forms in alkaline conditions.

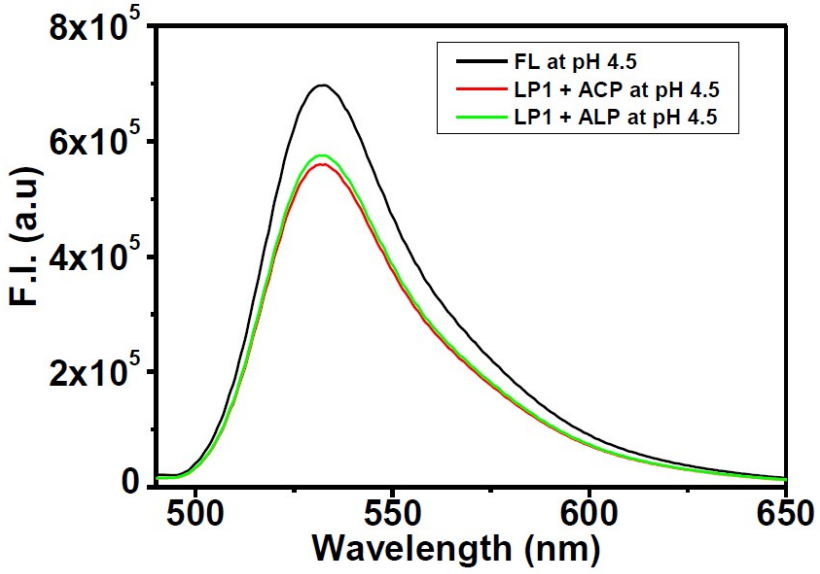


**Fig. S6.** Comparative Fluorescence study of **LP1** (10 μM) with Acid Phosphatase (500 ng/mL) (red line) and ALP (500ng/mL) (green line) in HEPES Buffer solution (0.01M) at pH 4.5 at 37°C. Fluorescence spectrum of **FL** at pH 4.5 (black line). Excitation at 490 nm and emmission at 532 nm respectively. Excitation and emission slit widths both set at 5 nm.

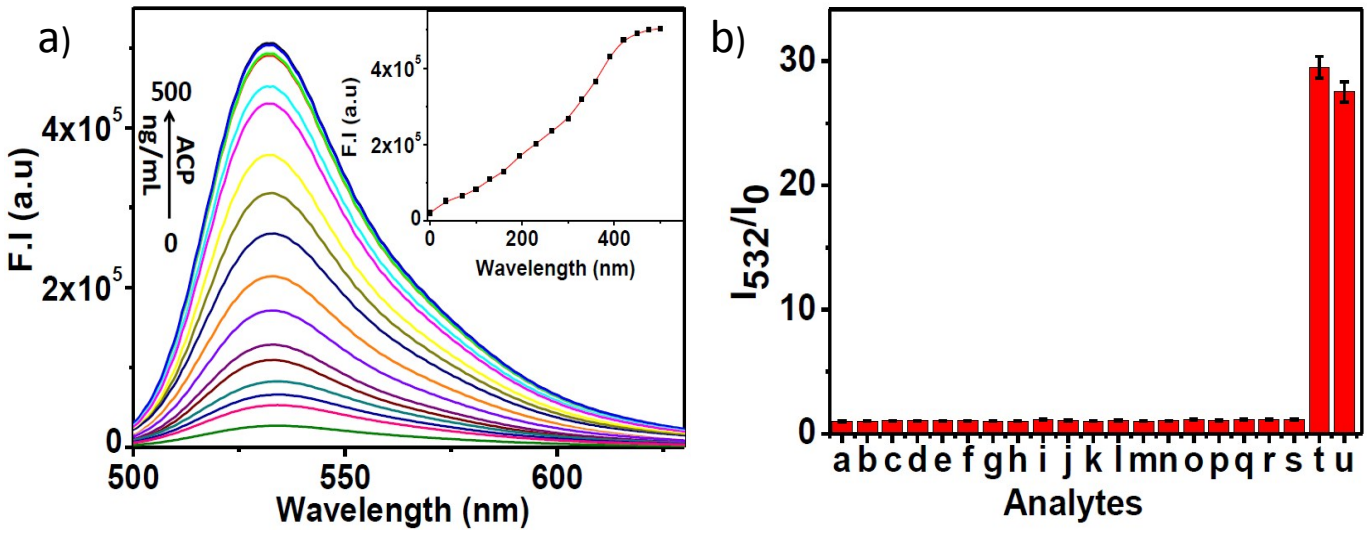


**Fig. S7.** Fluorescence study of LP1 (10 μM ) with (0-500 ng/mL) ACP at pH-4.5 in HEPES buffer solution at 37°C. b) Various analytes (500 μM) with LP1(10 μM ) a) $Fe^{3+}$, b) $Cu^{2+}$ , c) $Zn^{2+}$ , d) $Mg^{2+}$, e) $Ca^{2+}$, f) $Fe^{2+}$, g) $Na^{+}$, h) $K^{+}$ , i) $Cu^{+}$, j) $H_2O_2$, k) $NO_2^{-}$, l) $NO_3^{-}$ , m) GSH , n) ascorbic acid, o) cysteine, p) trypsin, q) pepsin, r) lipase, s) esterase, t) ALP (500 ng/mL) and u) ACP (500 ng/mL) at pH-4.5 in HEPES buffer solution at 37°C. All the data were acquired 30 min after addition of analytes at 37°C. Excitation at 490 nm and emission at 532 nm respectively. Excitation and emission slit widths both set at 5 nm.

***Detection limit ACP***

The Fluorescence titration was used to calculate the detection limit. The fluorescence emission spectrum of probe **LP1** ($2.0\times10^{-6}$ M) was measured ten times and the standard deviation of blank measurement was achieved. The fluorescence intensity at 532 nm was

plotted as a concentration of ACP. The detection limit was calculated by using following equation.

*Detection Limit 3σ/k*

Where σ is the standard deviation of blank measurement, k is the slope between the fluorescence intensity versus ACP concentration. We calculated lower detection limit toward phosphatase by applying regression equation; it was found to be 2.160 ng/mL (0.007 U/L ).

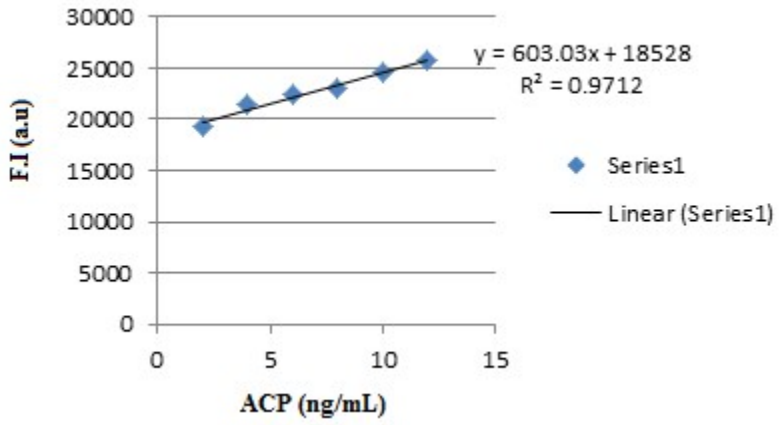


**Fig. S8.** The changes in the fluorescence intensity of **LP1** (2.0 μM) at 532 nm against varied concentrations of ACP from 0 to 15 ng/mL in HEPES buffer (0.01 M, pH 4.5) with the slit width 5/5 nm.

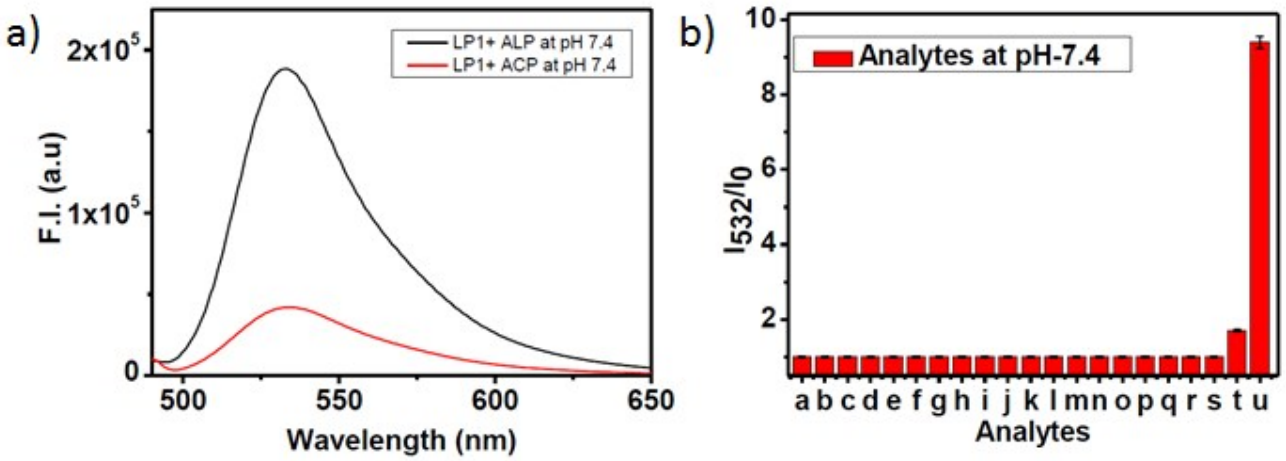


**Fig. S9.** a) Comparative Fluorescence study of **LP1** (10 μM) with Acid Phosphatase (500 ng/mL) (red line) and ALP (500ng/mL) (black line) in HEPES Buffer solution (0.01M) at pH 7.4 at 37°C. b) Various analytes (500 μM) of cations and anions tests with LP1(10 μM ) a) $Fe^{3+}$, b) $Cu^{2+}$ , c) $Zn^{2+}$ , d) $Mg^{2+}$, e) $Ca^{2+}$, f) $Fe^{2+}$, g) $Na^{+}$, h) $K^{+}$ , i) $Cu^{+}$, j) $H_2O_2$, k) $NO_2^-$, l) $NO_3^-$ , m) GSH , n) ascorbic acid, o) cysteine, p) trypsin, q) pepsin, r) lipase, s) esterase, t) ACP (500 ng/mL), u) ALP (500ng/mL) at pH-7.4 in HEPES buffer solution (0.01M) at 37 °C. All the data were acquired 30 min after addition of analytes at 37°C. Excitation at 490 nm and emmission at 532 nm respectively. Excitation and emission slit widths both set at 5 nm.

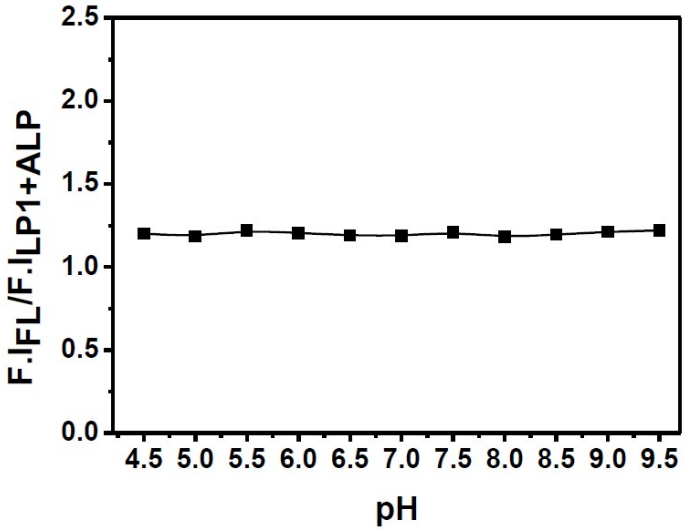


**Fig. S10.** Comparative Fluorescent intensity ratio between **FL** (10.0 μM ) and **LP1** (10.0 μM ) with ALP (500 ng/mL) at 37°C over a range of pH values (4.5–9.5) in HEPES buffer solution. All the data were acquired 30 min after addition of ALP at 37°C. Excitation at $\lambda_{ex}$ 490 nm and emission at $\lambda_{em}$ 532 nm respectively. Excitation and emission slit widths both set at 5 nm.

***Theoretical calculations***

*Computational details*

The hybrid density functional B3LYP was utilized for all calculations with the basis set 6-31G (d,p) as such in the Gaussian 16 program suite.[1] From the existing literature, such calculations have been done for Rhodamine type of molecules using the aforementioned basis set.[2] We performed all the calculations for neutral ions, cations and anions with the same geometry, density functional and basic set. The population's analysis was carried out with Hirshfeld population analysis (stockholders charge-partitioning method).

Conceptual DFT study of Lysosomal probe with Fukui function

Theoretical DFT used to create the chemical reactivity descriptors for the molecules. From these descriptors, we could analyze their global and local behaviors. In general, it gave the nucleophilicity and electrophilicity of the molecule which further extended to the predictability of nucleophile and electrophilic attack on the molecule. The hydrolyzed lysosomal probe (**FL**) was structurally similar to half of rhodamine and half of fluorescein. Due to this combination in its structure, it showed unique optical property both in UV-Vis spectrum and fluorescence spectrum concerning the pH of the medium. If the pH of the medium was alkaline, it showed less absorbance and fluorescence. If the pH of the medium was acidic, it showed high absorbance and fluorescence. Acidic pH was due to the formation of more $H^+$ ion which acts as an electrophile. In our theoretical study, we tried to analyze the electrophilic attack of $H^+$ ion on the lysosomal probe by using DFT and conceptual DFT. The **FL1** in an aqueous environment formed predominantly in cationic, zwitterion and lactonic form. From the literature [2], rhodamine and fluorescein dye molecule stayed in the form of a cationic and zwitterion. Here, we studied the aforementioned three forms by using DFT. HOMO-LUMO illustration of the lysosomal probe in cationic, zwitterion and lactonic forms is shown in Fig. 3. HOMO-LUMO pair of cationic form was entirely different of zwitterion and lactonic form. In the cationic form of **FL**, HOMO electron density cloud concentrated on piperazine moiety and the LUMO electron density cloud concentrated over xanthene moiety. But in contrast, in lactonic and zwitterionic form of a lysosomal probe, HOMO electron density cloud localized in between piperazine and xanthene moiety and the LUMO mainly shifted to phenyl lactone and phenyl carboxylate ion moieties respectively. Calculated values of the global hardness ($\eta$), global softness (S), the chemical potential ($\mu$), electrophilicity index ($\omega$), stabilization energy ($\Delta E$) of the lysosomal probe for all three different forms was given in the Table-S1. A cationic form of lysosomal probe showed high electrophilic index as compared to the other two form of a hydrolyzed lysosomal probe

(**FL**). From the stabilizing energy (ΔE), a cationic form of the lysosomal probe was much stable as compared with the other two forms of a lysosomal probe. The band gap between HOMO-LUMO was lower in the cationic form as compared with other two form of the fluorophore (**FL-1**) (table-1). It is due to the occurrence of more n-π* which was low in band gap as compare π-π* transition.

Fukui functional analysis was carried out for all these lysosomal probe forms. We calculated $f^+$ (which favors nucleophilic attack) and f-(which favors electrophilic attack). From this calculation, dual-descriptor (Δf) was estimated. If $\Delta f > 0$, a nucleophilic attack on the lysosomal probe was favored. If $\Delta f < 0$, an electrophilic attack on the lysosomal probe took place instead. For this analysis, we only focused on two nitrogen atom of piperazine moiety (N1-attached to the aliphatic carbon atom and N2-attached to the aromatic carbon atom of xanthene moiety) for all three form of the lysosomal probe. The cationic form of the lysosomal probe showed Δf=-0.080826 for N1 nitrogen atom and Δf=-0.004206 for N2 nitrogen atom of the piperazine moiety. The electrophilic attack of H+ ion was most favorable in the nitrogen (N1) atom which was attached to the aliphatic carbon. Therefore, the aromatic carbon attached nitrogen (N2) was able to transfer its lone pair of the electron (n) to an aromatic xanthene moiety (π*) during the excitation process (figure.2a) i.e. it favored a n-π* transitions. The zwitterion form of a lysosomal probe, it showed Δf=-0.011503 for N1 nitrogen atom and Δf=-0.09894 for N2 nitrogen atom of the piperazine moiety. The electrophilic attack of H+ ion was more favorable in the nitrogen (N2) atom that was attached to the aromatic carbon. The lactonic form of a lysosomal probe showed Δf=-0.021308for N1 nitrogen atom and Δf=-0.088633 for N2 nitrogen atom of the piperazine moiety. The electrophilic attack of $H^+$ ion was more favorable in the nitrogen (N2) atom that was attached to the aromatic carbon.

Moreover, a lactonic form of the lysosomal probe was not stable in the acid and alkaline medium; it could be either the cationic or zwitterionic forms of the hydrolyzed lysosomal probe (**FL**)

in acid and alkaline medium under equilibrium condition. They stayed in equilibrium in the aqueous medium. Zwitterionic form of lysosomal probe played a very critical role in the tunability of optical properties concerning the pH of the medium. In the alkaline medium, cationic form of lysosomal probe (**FL**) shifted its equilibrium to more zwitterionic form which gave less absorbance and less fluorescence emission intensity. In the acid medium, the zwitterionic form of lysosomal probe shifted its equilibrium to more cationic form which gave high absorbance and high fluorescence emission intensity (scheme-S2).

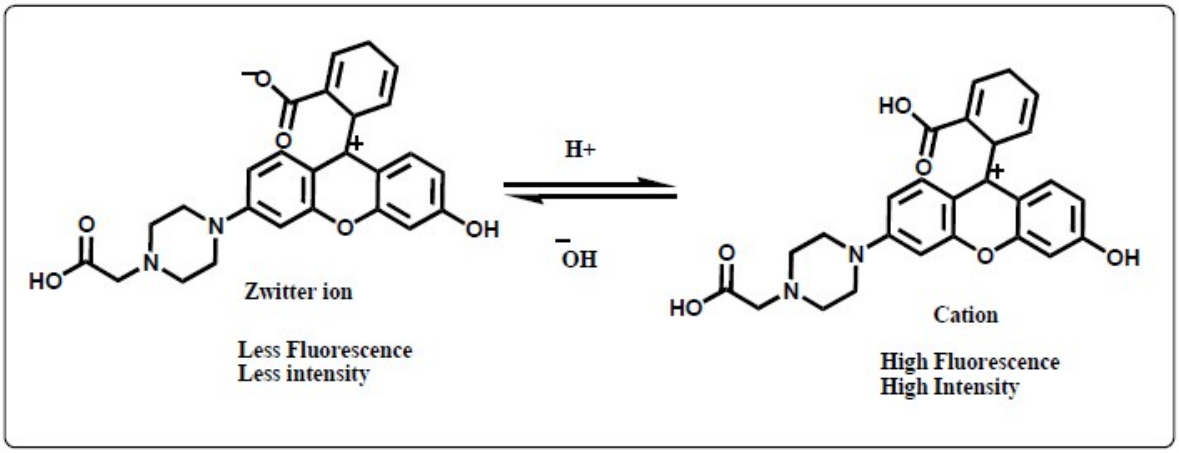


**Scheme S2:** The schematic representation of cationic and zwitterion form of lysosomal with respect to acid and alkaline pH.

***Theoretical Background***

From the conceptual density functional theory (DFT), various global chemical reactivity descriptors of the molecule such as global hardness (η),the global softness (S),the chemical potential (μ), the electrophilicity index (ω), the stabilization energy (ΔE) are given as theoretical establishments. The theoretical definition of the chemical potential (μ) was given by Parr et.al, [3]

$$- \mu = \frac{1}{2}(IP + EA) \quad \textbf{1}$$

Where IP is the ionization potential and EA represents the electron affinity,

$$- E_{HOMO} = IP \quad \textbf{2}$$

$$- E_{LUMO} = EA \quad \textbf{3}$$

According to eqn. (1), one could relate chemical potential (μ) of the molecule to the molecular orbital energies such as HOMO-LUMO pair. From the molecular orbital theory, IP and EA can be denoted by HOMO-LUMO energies.

The hardness of the molecule could be calculated by the Koopmanns' approximation as follows .[4]

$$\eta = IP - EA \quad \textbf{4}$$

From which a the local softness could be calculated as

$$S = \frac{1}{\eta} \quad \textbf{5}$$

The hardness could be described as a protection from charge exchange in the molecular environment, while the softness quality of the molecule measures the simplicity for substitution reaction with charge transfer. The inverse of the global hardness was known as the global softness.

The amount of electrophilic nature of the molecule (ω) was known as the "electrophilicity index". This was defined by Parr et al.,[3] as follows

$$\omega = \frac{\mu^2}{2\eta} \quad \textbf{6}$$

From which the stabilization energy given could be calculated as,

$$\Delta E = - \omega \quad \textbf{7}$$

From the eqn. (7) ΔE gave only negative value, the charge exchange of the molecule was an ideal process.[5] The numerator ($\mu^2$) is quadratic and, hence it becomes positive in nature and the denominators (2η) are sure because of the convexity of the energy vs. N curve.

Fukui functions could be written with finite approximation and frontier-orbital theory[6] for chemical reactivity as follows,

For the nucleophilic attack,

$$f^+ = \rho(N+1) - \rho(N) \quad \mathbf{9}$$

For an electrophilic attack,

$$f^- = \rho(N) - \rho(N-1) \quad \mathbf{10}$$

Morelle et al.[7] gave a new index of selectivity toward an electrophilic and nucleophilic attack in the same. This index was denoted as dual-descriptor and described as follows,

$$\Delta f = f^+ - f^- \quad \mathbf{11}$$

When $\Delta f > 0$, the atom undergoes a nucleophilic attack, whereas if $\Delta f < 0$, the atom undergoes an electrophilic attack.

| S.No | **FL** | values | | | | | |
|---|---|---|---|---|---|---|---|
| | | η | S | μ | ω | ΔE | (eV) |
| 1. | Cation | 0.39267 | 2.546668 | -0.241275 | 0.074125 | -0.074125 | 2.679526252 |
| 2. | Zwitterion | 0.38416 | 2.603082 | -0.1302 | 0.022064 | -0.022064 | 4.07357652 |
| 3. | Lactonic | 0.38059 | 2.627499 | -0.12955 | 0.022047 | -0.022047 | 4.264874068 |

**Table S2:** Calculated values of the global hardness (η),global softness (S),chemical potential (μ), electrophilicity index (ω), stabilization energy (ΔE) of and HOMO-LUMO band gap (eV) of FL.

| **Atoms** | **Label no** | **P Anion** | **P Cation** | **Neutral** | **(Δf)** |
|---|---|---|---|---|---|
| C | 1 | 6.013183 | 5.989388 | 6.007392 | -0.012213 |
| C | 2 | 5.998337 | 5.97684 | 5.99075 | -0.006323 |
| C | 3 | 5.998357 | 5.976268 | 5.990784 | -0.006943 |
| C | 4 | 6.013837 | 5.990185 | 6.008652 | -0.013282 |
| H | 5 | 0.96652 | 0.93396 | 0.953856 | -0.007232 |
| H | 6 | 0.955476 | 0.936687 | 0.95058 | -0.008997 |
| H | 7 | 0.971519 | 0.931529 | 0.95473 | -0.006412 |
| H | 8 | 0.976309 | 0.946498 | 0.97314 | -0.023473 |
| N | 9 | 7.103941 | 7.018221 | 7.101494 | -0.080826 |
| N | 10 | 7.049938 | 6.965392 | 7.009768 | -0.004206 |
| C | 11 | 5.954589 | 5.904894 | 5.910906 | 0.037671 |
| C | 12 | 6.079574 | 6.022026 | 6.040474 | 0.020652 |
| C | 13 | 6.093483 | 6.035002 | 6.073376 | -0.018267 |
| C | 14 | 6.05185 | 5.992072 | 6.011138 | 0.021646 |
| H | 15 | 0.968019 | 0.935473 | 0.946224 | 0.011044 |
| C | 16 | 5.919746 | 5.87965 | 5.890028 | 0.01934 |
| H | 17 | 0.962874 | 0.931783 | 0.945784 | 0.003089 |
| C | 18 | 6.032881 | 5.98721 | 6.015434 | -0.010777 |
| H | 19 | 0.964283 | 0.929494 | 0.943252 | 0.007273 |
| C | 20 | 6.021383 | 5.913427 | 5.931792 | 0.071226 |
| C | 21 | 5.977595 | 5.999464 | 5.989564 | -0.002069 |
| C | 22 | 6.016181 | 6.012348 | 6.012498 | 0.003533 |
| C | 23 | 6.035038 | 6.030081 | 6.030836 | 0.003447 |
| C | 24 | 6.032998 | 6.006306 | 6.016282 | 0.00674 |
| C | 25 | 6.029693 | 6.001718 | 6.01214 | 0.007131 |
| H | 26 | 0.952047 | 0.945736 | 0.947104 | 0.003575 |

| | | | | | |
|---|---|---|---|---|---|
| C | 27 | 6.041649 | 6.004017 | 6.018406 | 0.008854 |
| H | 28 | 0.956148 | 0.933994 | 0.94224 | 0.005662 |
| H | 29 | 0.953479 | 0.928936 | 0.938122 | 0.006171 |
| H | 30 | 0.954935 | 0.927611 | 0.938216 | 0.006114 |
| C | 31 | 6.027065 | 5.99025 | 6.016034 | -0.014753 |
| C | 32 | 5.916908 | 5.877896 | 5.890526 | 0.013752 |
| C | 33 | 6.050709 | 5.991471 | 6.010072 | 0.022036 |
| C | 34 | 6.079953 | 6.040035 | 6.05532 | 0.009348 |
| C | 35 | 6.082766 | 6.016328 | 6.047492 | 0.00411 |
| H | 36 | 0.963325 | 0.930743 | 0.943162 | 0.007744 |
| C | 37 | 5.929672 | 5.855498 | 5.8834 | 0.01837 |
| H | 38 | 0.950382 | 0.918536 | 0.930326 | 0.008266 |
| H | 39 | 0.965074 | 0.923791 | 0.941246 | 0.006373 |
| C | 40 | 5.794469 | 5.787685 | 5.790286 | 0.001582 |
| O | 41 | 8.264445 | 8.270653 | 8.267388 | 0.000322 |
| O | 42 | 8.174847 | 8.144838 | 8.1572 | 0.005285 |
| H | 43 | 0.812877 | 0.794653 | 0.801234 | 0.005062 |
| O | 44 | 8.09837 | 8.048592 | 8.061126 | 0.02471 |
| O | 45 | 8.19283 | 8.114488 | 8.150584 | 0.00615 |
| H | 46 | 0.966778 | 0.933714 | 0.954168 | -0.007844 |
| H | 47 | 0.956653 | 0.935463 | 0.951102 | -0.010088 |
| H | 48 | 0.975983 | 0.946629 | 0.972662 | -0.022712 |
| H | 49 | 0.971027 | 0.932102 | 0.954882 | -0.006635 |
| C | 50 | 6.005869 | 5.984616 | 6.001914 | -0.013343 |
| H | 51 | 0.952558 | 0.92582 | 0.945644 | -0.01291 |
| H | 52 | 0.95235 | 0.925904 | 0.945632 | -0.01301 |
| C | 53 | 5.791042 | 5.7715 | 5.788894 | -0.015246 |
| O | 54 | 8.265476 | 8.238778 | 8.268316 | -0.032378 |
| O | 55 | 8.179585 | 8.141162 | 8.169948 | -0.019149 |
| H | 56 | 0.812704 | 0.787169 | 0.80594 | -0.012007 |
| H | 57 | 0.820422 | 0.785476 | 0.80055 | 0.004798 |

**Table S3.** The population and duel descriptor (Δf) of thecationic structure of FL.

| **Atoms** | **Label no** | **P Anion** | **P Cation** | **Neutral** | **(Δf)** |
|---|---|---|---|---|---|
| C | 1 | 6.013908 | 6.000435 | 6.011342 | -0.008341 |
| C | 2 | 6.007769 | 5.989224 | 6.004796 | -0.012599 |
| C | 3 | 6.006543 | 5.987051 | 6.003418 | -0.013242 |

| | | | | | |
|---|---|---|---|---|---|
| C | 4 | 6.014797 | 6.002563 | 6.012502 | -0.007644 |
| H | 5 | 0.972028 | 0.94678 | 0.965312 | -0.011816 |
| H | 6 | 0.962701 | 0.944161 | 0.959514 | -0.012166 |
| H | 7 | 0.983218 | 0.94384 | 0.976854 | -0.02665 |
| H | 8 | 0.978975 | 0.961728 | 0.976648 | -0.012593 |
| N | 9 | 7.105716 | 7.080452 | 7.103738 | -0.021308 |
| N | 10 | 7.077244 | 6.974551 | 7.070214 | -0.088633 |
| C | 11 | 5.965244 | 5.924937 | 5.948694 | -0.007207 |
| C | 12 | 6.079388 | 6.01362 | 6.063742 | -0.034476 |
| C | 13 | 6.090303 | 6.047646 | 6.078412 | -0.018875 |
| C | 14 | 6.03198 | 6.008537 | 6.03516 | -0.029803 |
| H | 15 | 0.969642 | 0.936806 | 0.959136 | -0.011824 |
| C | 16 | 5.935324 | 5.894844 | 5.923764 | -0.01736 |
| H | 17 | 0.968335 | 0.939537 | 0.958158 | -0.008444 |
| C | 18 | 6.034802 | 5.973956 | 6.042154 | -0.07555 |
| H | 19 | 0.954003 | 0.935509 | 0.956076 | -0.02264 |
| C | 20 | 5.914041 | 5.90746 | 5.910082 | 0.001337 |
| C | 21 | 6.035024 | 6.00801 | 6.000888 | 0.041258 |
| C | 22 | 6.07672 | 6.020343 | 6.023426 | 0.050211 |
| C | 23 | 6.073929 | 6.032823 | 6.033624 | 0.039504 |
| C | 24 | 6.075093 | 6.007477 | 6.020872 | 0.040826 |
| C | 25 | 6.107984 | 6.014425 | 6.026968 | 0.068473 |
| H | 26 | 0.975653 | 0.94881 | 0.950094 | 0.024275 |
| C | 27 | 6.075473 | 6.015871 | 6.03548 | 0.020384 |
| H | 28 | 0.972963 | 0.932266 | 0.943182 | 0.018865 |
| H | 29 | 0.990769 | 0.941348 | 0.9521 | 0.027917 |
| H | 30 | 0.981627 | 0.939152 | 0.952594 | 0.015591 |
| C | 31 | 6.032563 | 6.036882 | 6.03873 | -0.008015 |
| C | 32 | 5.932752 | 5.920765 | 5.91905 | 0.015417 |
| C | 33 | 6.038389 | 6.014395 | 6.031572 | -0.01036 |
| C | 34 | 6.095589 | 6.046488 | 6.071286 | -0.000495 |
| C | 35 | 6.09714 | 6.054257 | 6.074584 | 0.002229 |
| H | 36 | 0.955495 | 0.94398 | 0.954026 | -0.008577 |
| C | 37 | 5.935628 | 5.897608 | 5.917676 | -0.002116 |
| H | 38 | 0.962374 | 0.934268 | 0.946332 | 0.003978 |
| H | 39 | 0.97343 | 0.943392 | 0.95848 | -0.000138 |
| C | 40 | 5.865373 | 5.803703 | 5.808778 | 0.05152 |
| O | 41 | 8.357917 | 8.248874 | 8.279248 | 0.048295 |
| O | 42 | 8.175733 | 8.132868 | 8.140516 | 0.027569 |
| O | 43 | 8.116905 | 8.084441 | 8.105258 | -0.00917 |
| O | 44 | 8.209286 | 8.164842 | 8.189866 | -0.005604 |

| | | | | | |
|---|---|---|---|---|---|
| H | 45 | 0.971892 | 0.947007 | 0.965556 | -0.012213 |
| H | 46 | 0.962567 | 0.946021 | 0.96081 | -0.013032 |
| H | 47 | 0.978905 | 0.961357 | 0.976246 | -0.01223 |
| H | 48 | 0.983329 | 0.945585 | 0.97728 | -0.025646 |
| C | 49 | 6.01278 | 5.997223 | 6.005238 | -0.000473 |
| H | 50 | 0.964387 | 0.940816 | 0.952398 | 0.000407 |
| H | 51 | 0.964188 | 0.940611 | 0.952302 | 0.000195 |
| C | 52 | 5.824807 | 5.784668 | 5.790864 | 0.027747 |
| O | 53 | 8.295326 | 8.258892 | 8.266602 | 0.021014 |
| O | 54 | 8.205191 | 8.167209 | 8.18367 | 0.00506 |
| H | 55 | 0.826285 | 0.802681 | 0.814784 | -0.000602 |
| H | 56 | 0.830599 | 0.807025 | 0.819936 | -0.002248 |

**Table S4.** The population and duel descriptor (Δf) of thelactonic structure of FL.

| Atoms | Label no | P Anion | P Cation | Neutral | (Δf) |
|---|---|---|---|---|---|
| C | 1 | 6.011262 | 5.999481 | 6.008704 | -0.00667 |
| C | 2 | 6.001451 | 5.981669 | 5.998142 | -0.01316 |
| C | 3 | 6.002952 | 5.984101 | 6.001058 | -0.01506 |
| C | 4 | 6.008049 | 5.995017 | 6.005764 | -0.00846 |
| H | 5 | 0.972694 | 0.946333 | 0.965062 | -0.0111 |
| H | 6 | 0.965332 | 0.939944 | 0.961018 | -0.01676 |
| H | 7 | 0.963236 | 0.943416 | 0.96068 | -0.01471 |
| H | 8 | 0.968665 | 0.946161 | 0.964504 | -0.01418 |
| N | 9 | 7.10923 | 7.091907 | 7.10632 | -0.0115 |
| N | 10 | 7.063723 | 6.950117 | 7.05639 | -0.09894 |
| C | 11 | 5.961514 | 5.92443 | 5.949212 | -0.01248 |
| C | 12 | 6.086341 | 6.021706 | 6.073296 | -0.03855 |
| C | 13 | 6.098747 | 6.040263 | 6.086414 | -0.03382 |
| C | 14 | 6.032369 | 6.00554 | 6.035876 | -0.03384 |
| H | 15 | 0.971018 | 0.938318 | 0.96221 | -0.01508 |
| C | 16 | 5.934313 | 5.897765 | 5.924894 | -0.01771 |
| H | 17 | 0.970281 | 0.937749 | 0.960288 | -0.01255 |
| C | 18 | 6.039132 | 5.974608 | 6.048346 | -0.08295 |
| H | 19 | 0.954358 | 0.934851 | 0.956994 | -0.02478 |
| C | 20 | 5.913759 | 5.9076 | 5.910438 | 0.000483 |
| C | 21 | 6.034682 | 6.00845 | 6.000472 | 0.042188 |
| C | 22 | 6.07674 | 6.020541 | 6.023556 | 0.050169 |
| C | 23 | 6.075417 | 6.033079 | 6.033642 | 0.041212 |

| | | | | | |
|---|---|---|---|---|---|
| C | 24 | 6.076634 | 6.008062 | 6.021498 | 0.0417 |
| C | 25 | 6.108998 | 6.014918 | 6.027666 | 0.068584 |
| H | 26 | 0.976212 | 0.94893 | 0.950208 | 0.024726 |
| C | 27 | 6.075359 | 6.016601 | 6.036268 | 0.019424 |
| H | 28 | 0.973525 | 0.93263 | 0.943666 | 0.018823 |
| H | 29 | 0.991258 | 0.941648 | 0.952596 | 0.027714 |
| H | 30 | 0.981823 | 0.939534 | 0.953138 | 0.015081 |
| C | 31 | 6.031601 | 6.036067 | 6.038704 | -0.00974 |
| C | 32 | 5.931329 | 5.92123 | 5.918816 | 0.014927 |
| C | 33 | 6.035776 | 6.018274 | 6.032044 | -0.01004 |
| C | 34 | 6.093437 | 6.054562 | 6.071962 | 0.004075 |
| C | 35 | 6.095664 | 6.054841 | 6.075528 | -0.00055 |
| H | 36 | 0.954571 | 0.945306 | 0.954444 | -0.00901 |
| C | 37 | 5.935382 | 5.898442 | 5.91836 | -0.0029 |
| H | 38 | 0.961663 | 0.936497 | 0.946886 | 0.004388 |
| H | 39 | 0.972814 | 0.944188 | 0.959026 | -0.00105 |
| C | 40 | 5.866943 | 5.804389 | 5.809404 | 0.052524 |
| O | 41 | 8.176634 | 8.133934 | 8.141602 | 0.027364 |
| O | 42 | 8.359966 | 8.250993 | 8.281386 | 0.048187 |
| O | 43 | 8.116783 | 8.091343 | 8.105898 | -0.00367 |
| O | 44 | 8.209218 | 8.166214 | 8.190684 | -0.00594 |
| H | 45 | 0.980085 | 0.961475 | 0.974806 | -0.00805 |
| H | 46 | 0.973376 | 0.93867 | 0.970144 | -0.02824 |
| H | 47 | 0.979661 | 0.966101 | 0.977894 | -0.01003 |
| H | 48 | 0.977995 | 0.938207 | 0.97134 | -0.02648 |
| C | 49 | 6.014994 | 5.999651 | 6.005868 | 0.002909 |
| H | 50 | 0.965962 | 0.93966 | 0.95094 | 0.003742 |
| H | 51 | 0.966023 | 0.940918 | 0.952058 | 0.002825 |
| C | 52 | 5.834988 | 5.787618 | 5.792006 | 0.038594 |
| O | 53 | 8.301563 | 8.269321 | 8.266804 | 0.037276 |
| O | 54 | 8.207361 | 8.165785 | 8.181108 | 0.01093 |
| H | 55 | 0.826628 | 0.802965 | 0.813566 | 0.002461 |
| H | 56 | 0.830518 | 0.807993 | 0.820412 | -0.00231 |

**Table S5.** The population and duel descriptor (Δf) of zwitterion structure of FL.

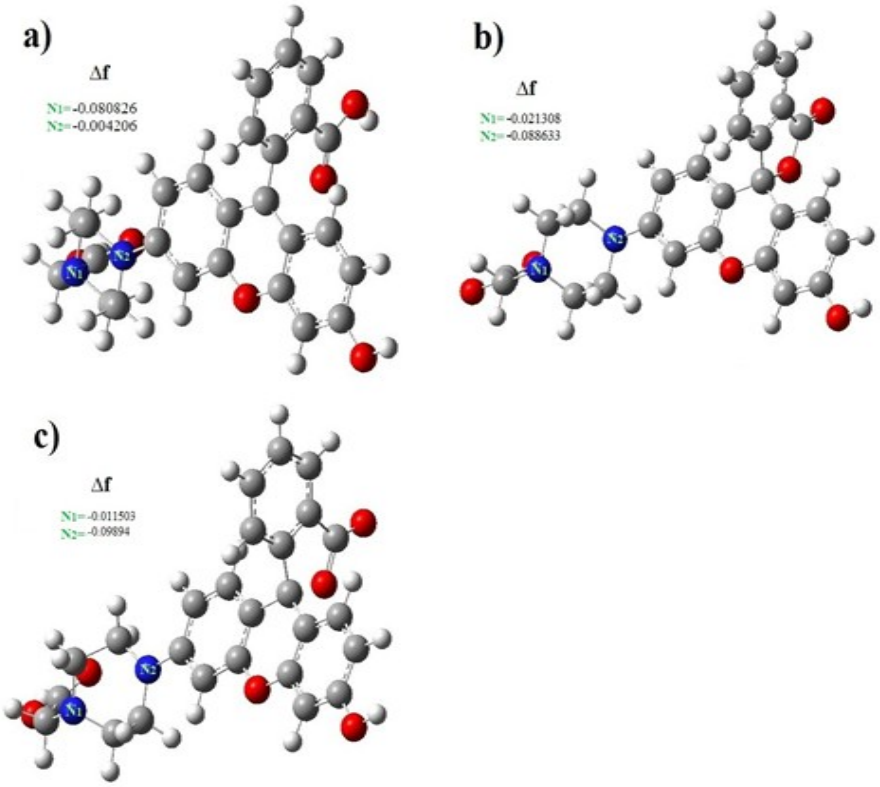


**Fig.S11.** Geometrically optimized structure and their Δf value (N1 and N2) for Lysosomal probe: a) cation form b) lactonic form c) zwitterion form.

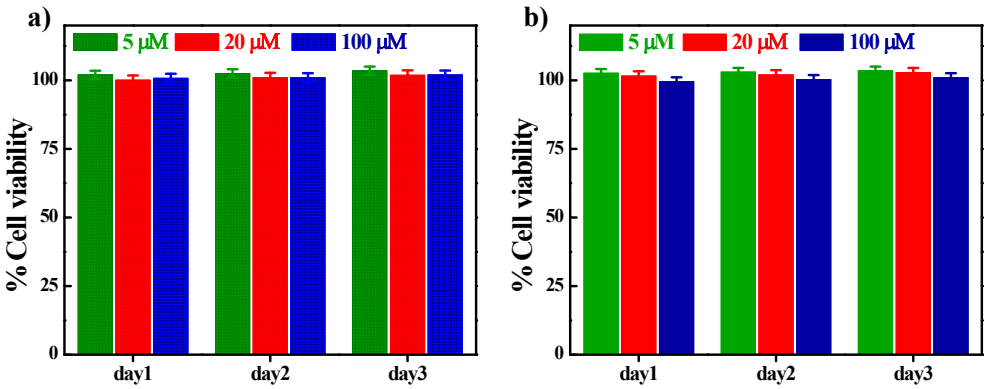


**Fig. S12.** Cytotoxicity of **LP1** on treatment in human cervical cancer (HeLa) cells and normal fibroblast (NIH-3T3) cells. a) NIH-3T3 and b) HeLa cells were seeded with varying concentration of **LP1**ranging from 5.0 µM to100.0 µM for 24 h, 48 h and 72 h followed by treatment with MTT and absorbance recorded at 570 nm. Viability values are measured against untreated control cells with medium alone; the results are presented with mean ± standard deviation (SD) values obtained from three independent experiments.

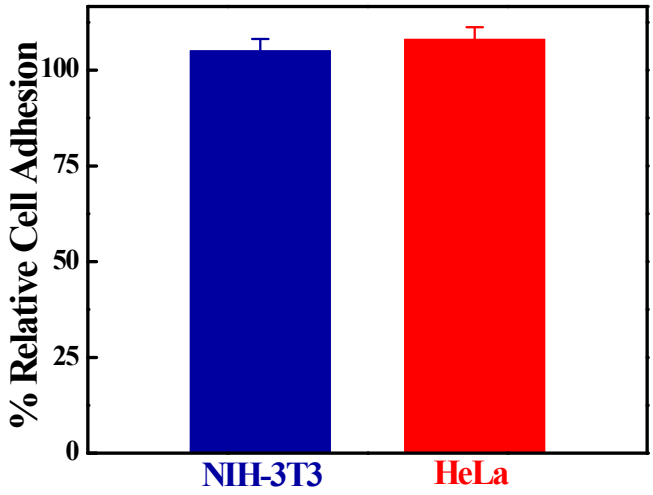


**Fig. S13.** Relative cells adhesion values of **LP1** using a modified crystal violet staining assay after 12 h incubation against NIH-3T3 and HeLa cells.

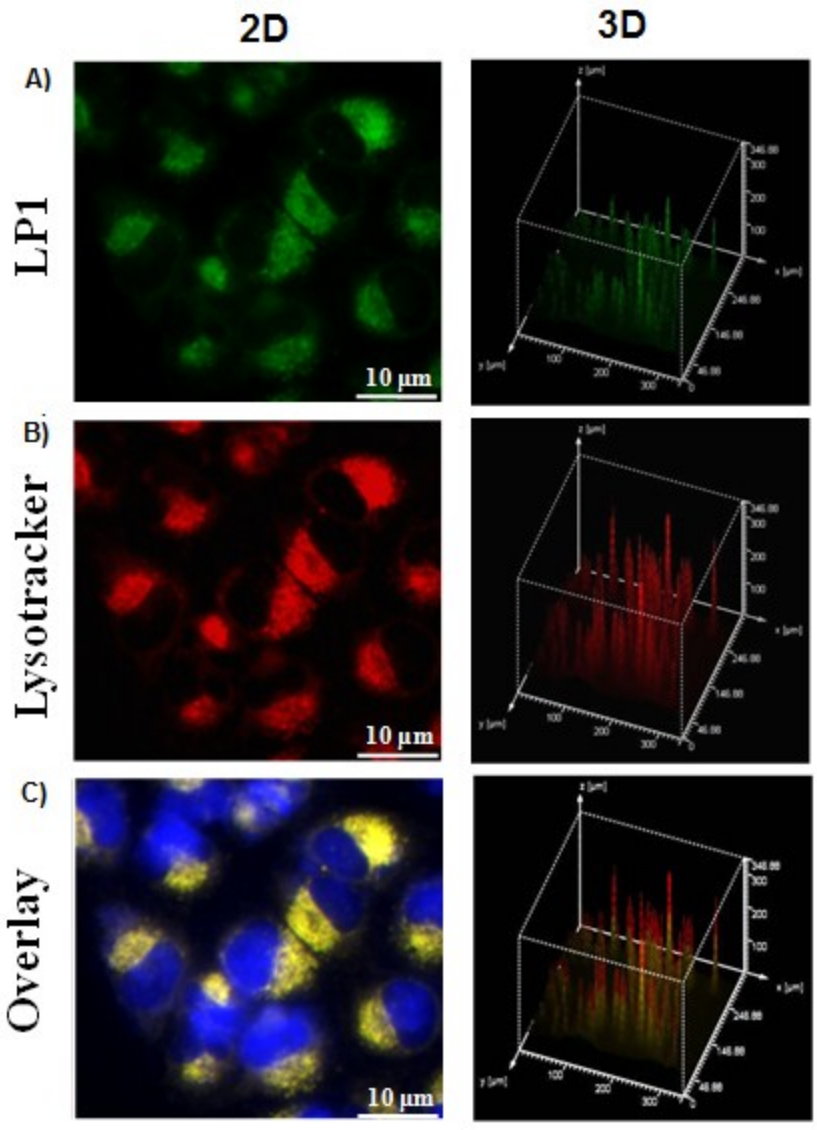


**Fig. S14.** 3D Co-localization images of **LP1** in HeLa Cell. **(A) LP1** in HeLa Cell, **(B)** Lysotracker in HeLa Cell and **(C)** Merged of **A** and **B** with nucleus. Images were taken at $\lambda_{ex}$ = 490 nm./ $\lambda_{ex}$ = 600 nm for **LP1** and Lysotracker red respectively. The value of colocalization coefficient (PC) (r = 0.93).

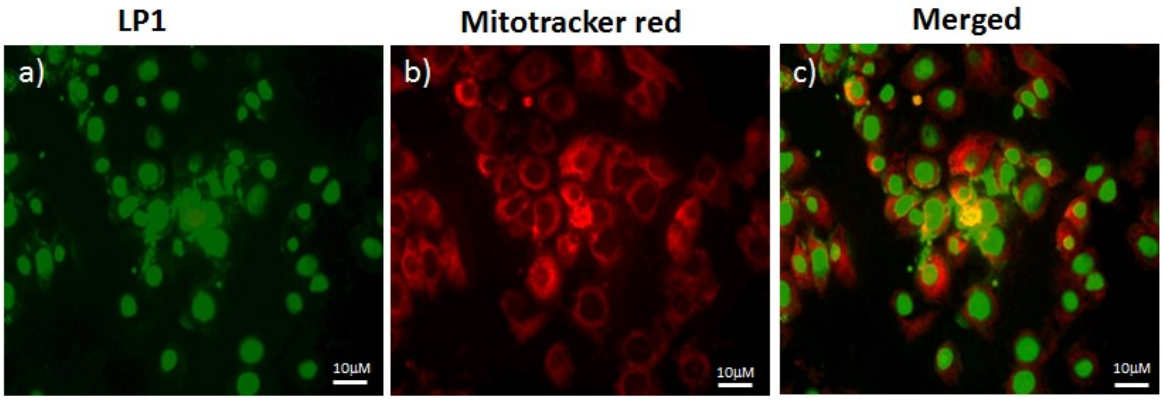


**Fig. S15.** Confocal fluorescence images of HeLa cells. a) The HeLa cells were incubated with **LP1** (5 μM) for 30 min and b) The HeLa cells were incubated with Mitotracker Red for 30 min. c) Merged image of a) and b). Images were taken at $\lambda_{ex}$/ $\lambda_{em}$ = 490 nm/540 nm for **LP1;** for mitotracker red $\lambda_{ex}$/ $\lambda_{em}$ = 590 nm/630 nm. Scale bar: 10 μm.

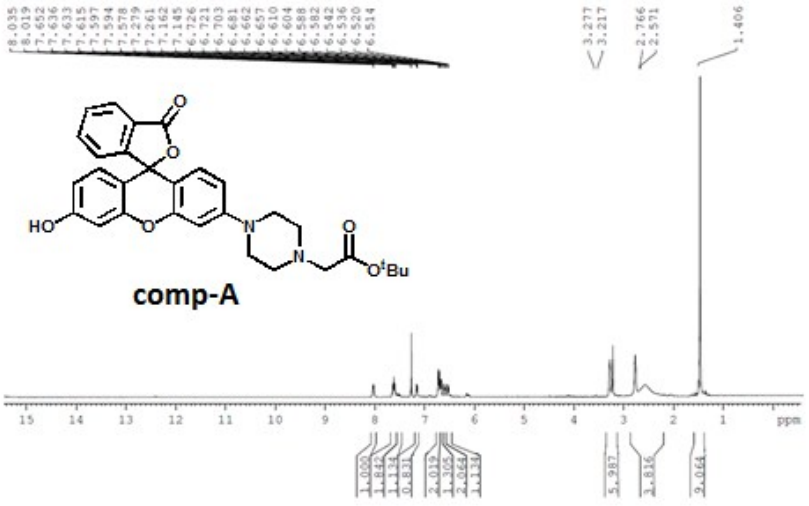


**Fig. S16.** $^{1}$**H-NMR** of **comp-A** in **DMSO-$d_6$.**

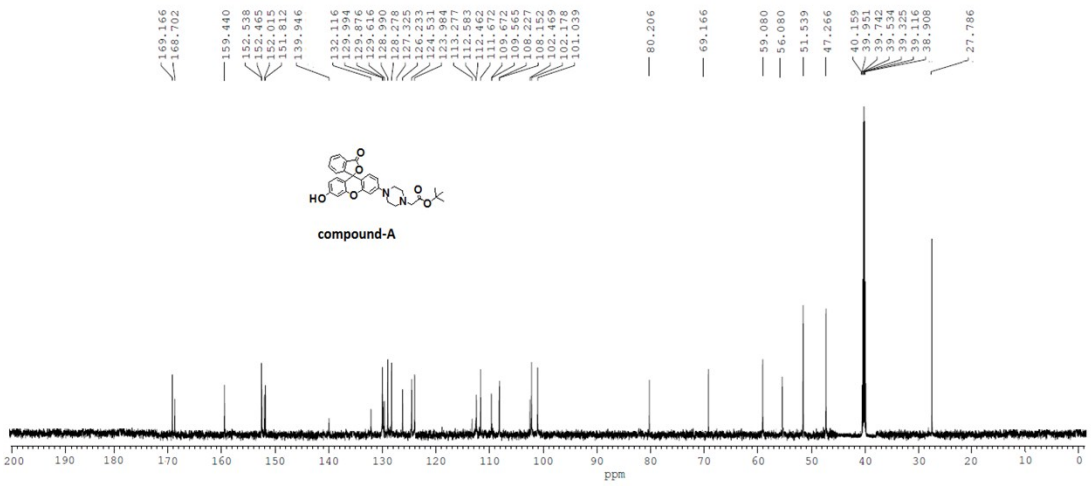


**Fig. S17.** $^{13}$**C-NMR** of **compound A** in **DMSO-*d*$_6$**

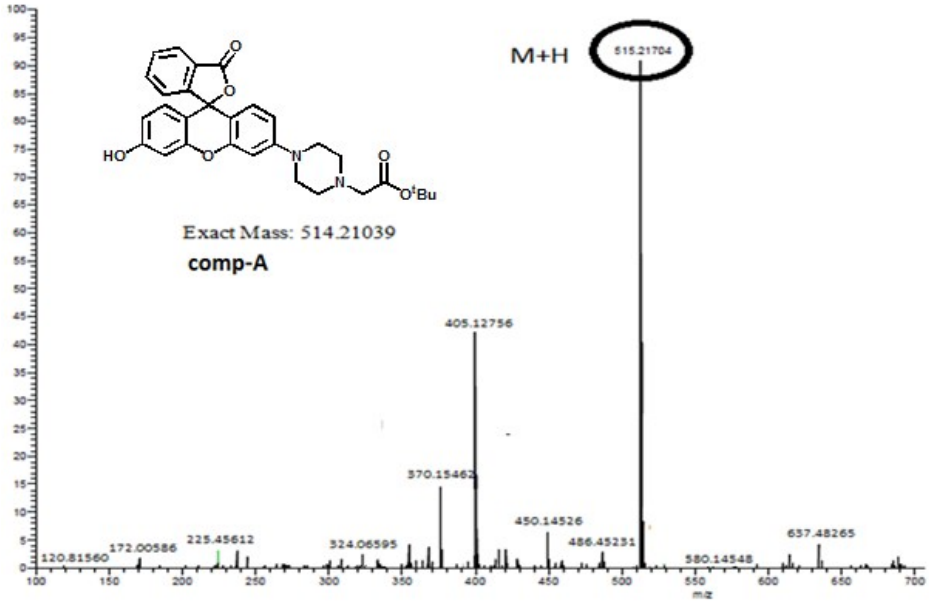


**Fig. S18. ESI-HRMS** of **comp-A.**

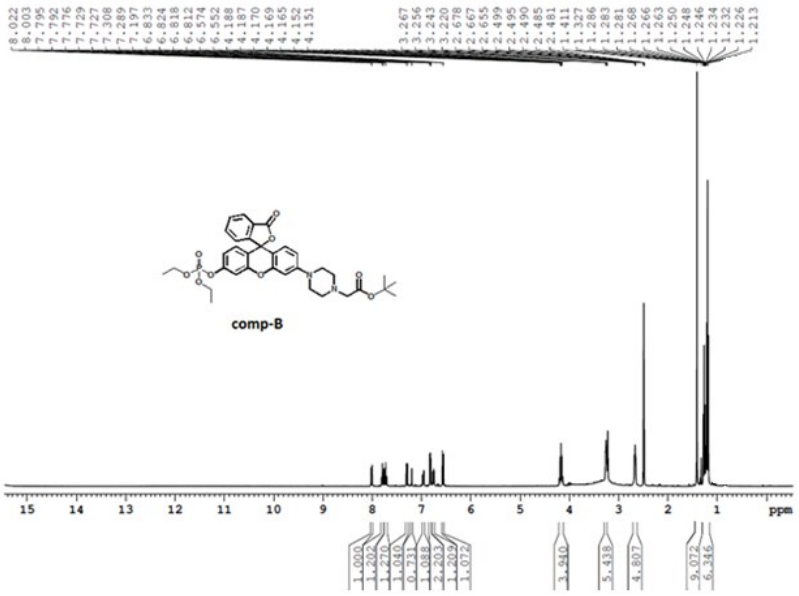


**Fig. S19. $^{1}$H-NMR** of **comp-B** in **DMSO-$d_6$.**

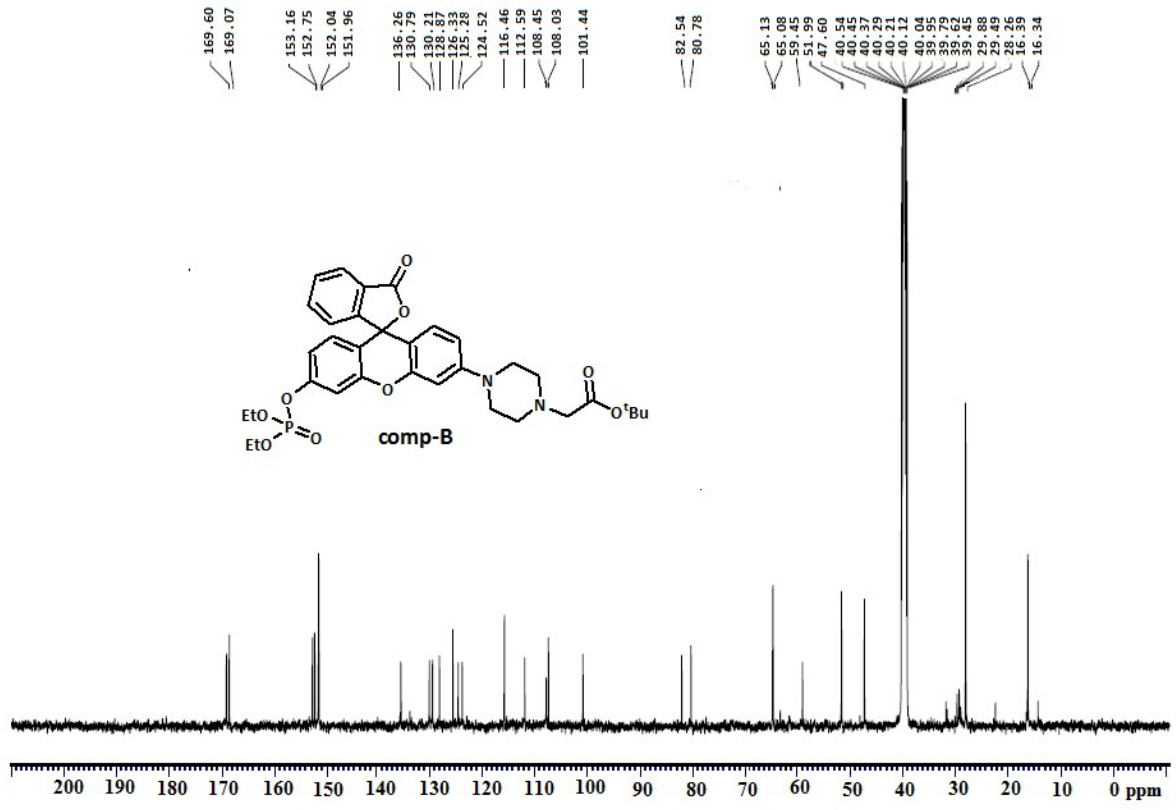


**Fig. S20. $^{13}$C-NMR** of **comp-B** in **DMSO-$d_6$**

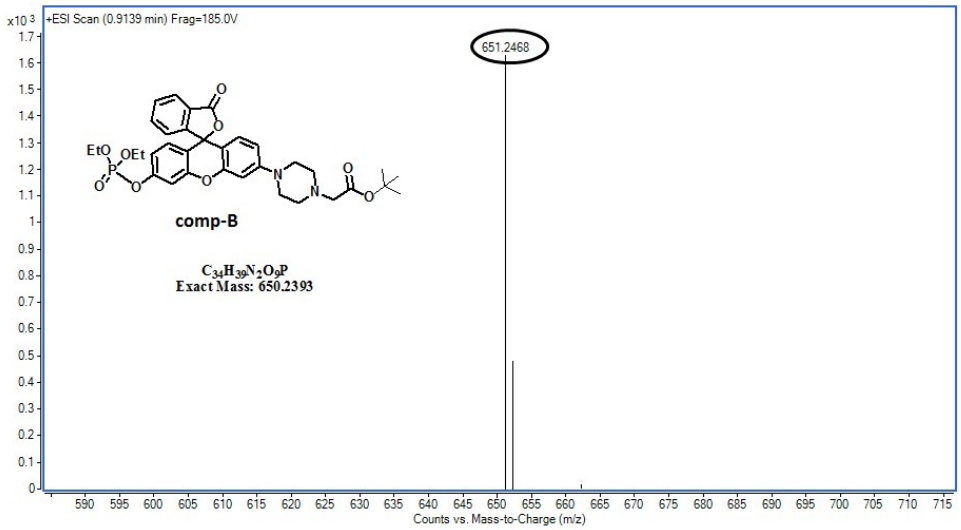


**Fig. S21. ESI-HRMS** of **comp-B.**

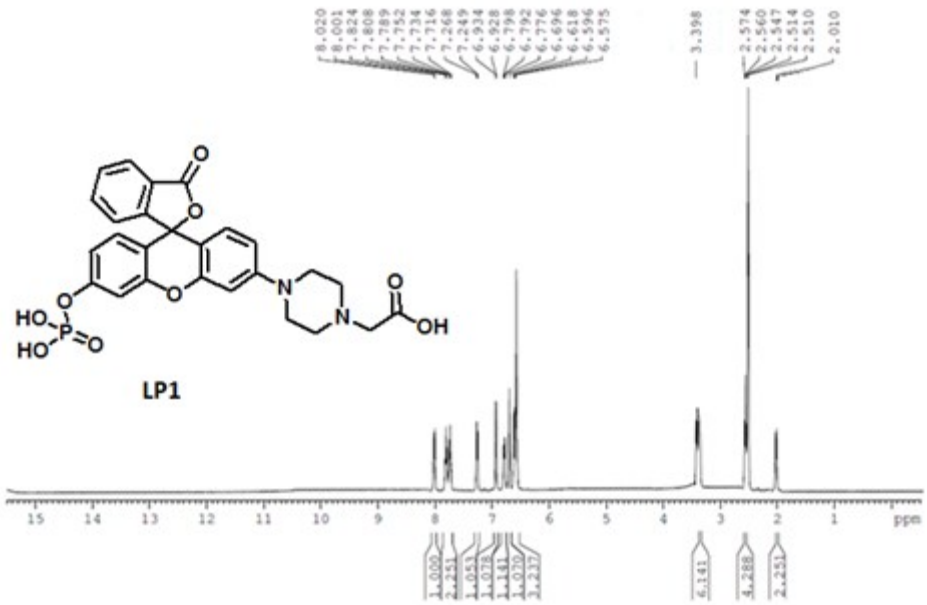


**Fig. S22. $^{1}$H-NMR** of **LP1** in **DMSO-*d*$_6$.**

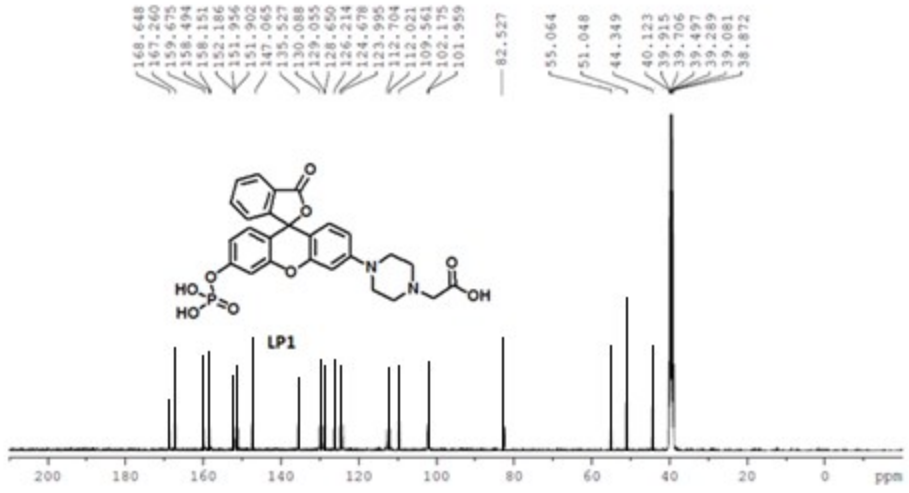


**Fig. S23. $^{13}$C-NMR** of **LP1** in **DMSO-$d_6$.**

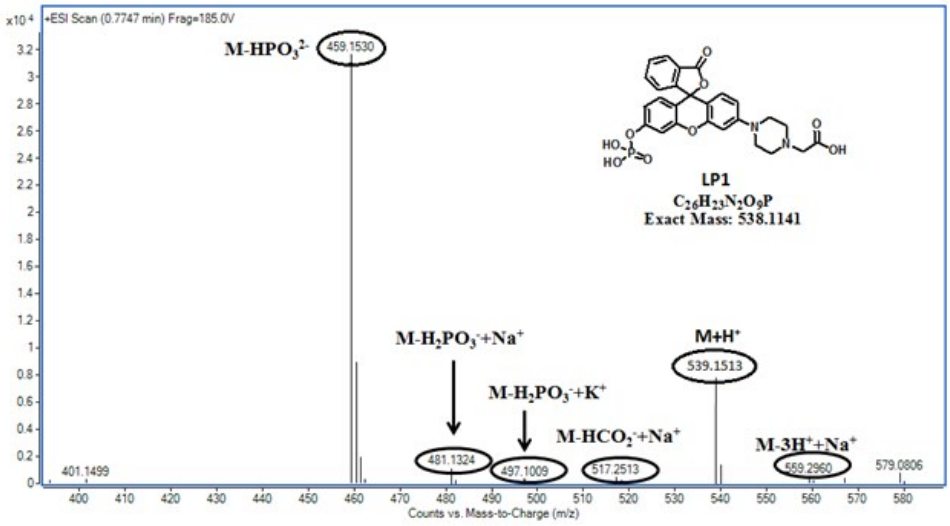


**Fig. S24. ESI-HRMS** of **LP1.**

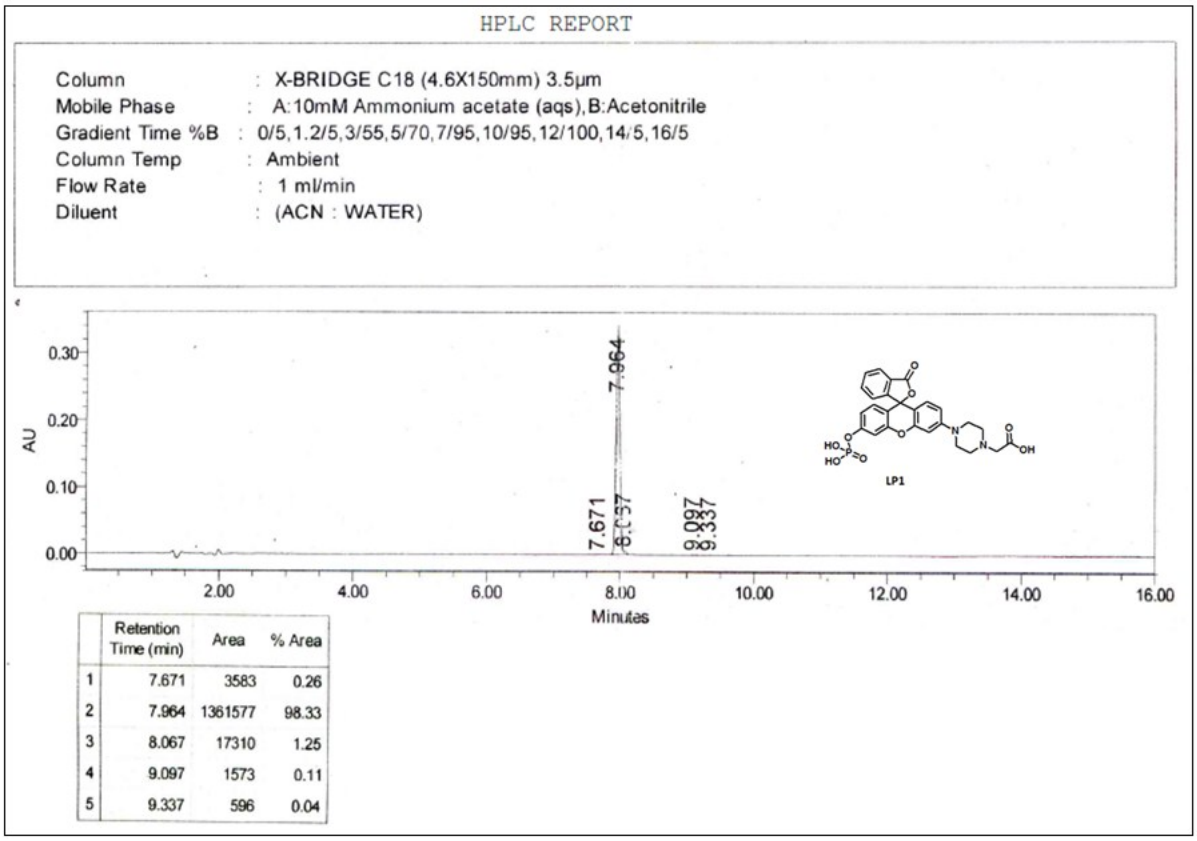


| | Retention Time (min) | Area | % Area |
|---|---|---|---|
| 1 | 7.671 | 3583 | 0.26 |
| 2 | 7.964 | 1361577 | 98.33 |
| 3 | 8.067 | 17310 | 1.25 |
| 4 | 9.097 | 1573 | 0.11 |
| 5 | 9.337 | 596 | 0.04 |

**Fig. S25: HPLC** of **LP1**.

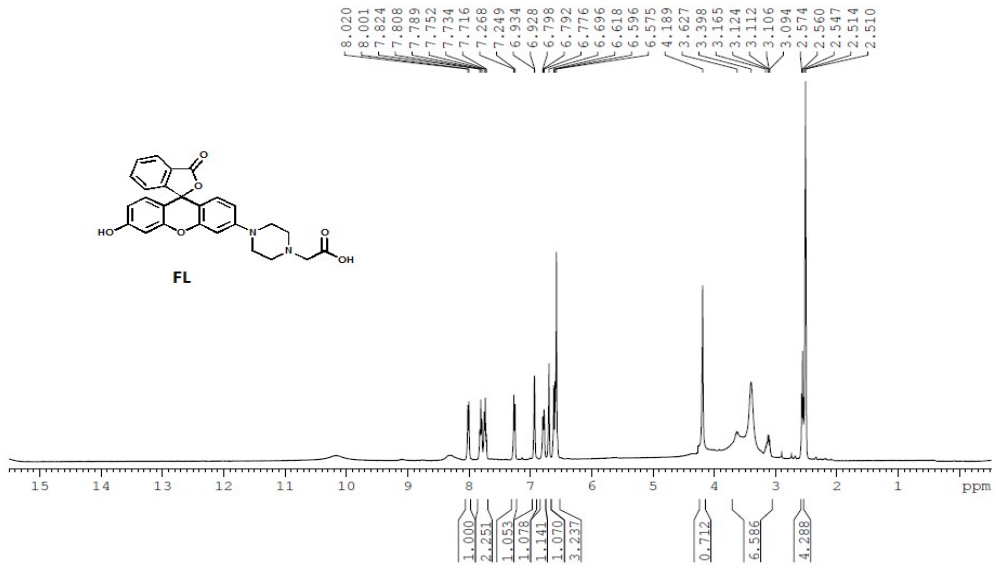


**Fig. S26. $^{1}$H-NMR** of **FL** in **DMSO-*d*$_6$.**

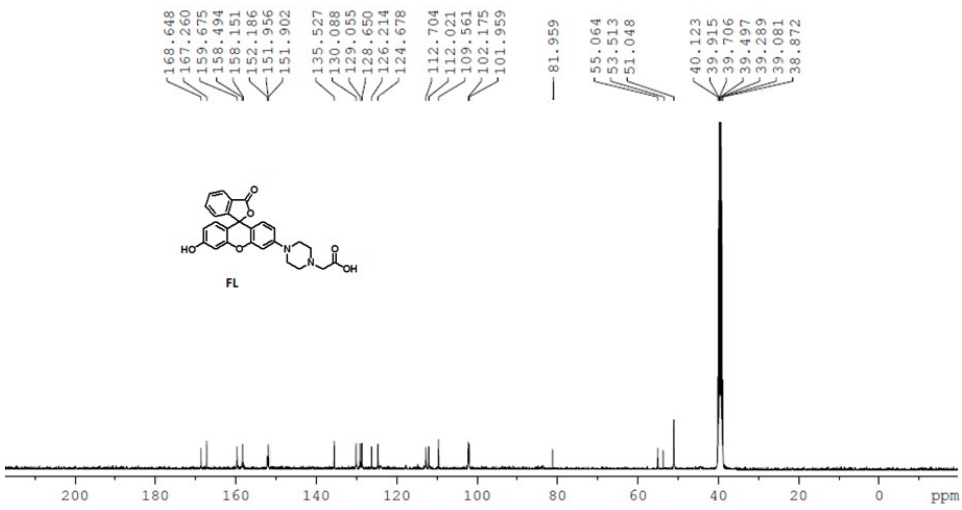


**Fig. S27. $^{13}$C-NMR** of **FL** in **DMSO-*d*$_6$**.

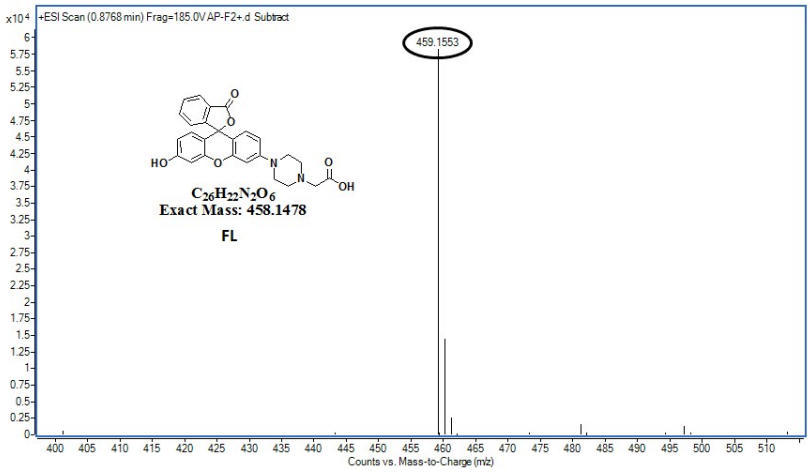


**Fig. S28. ESI-HRMS** of **FL.**

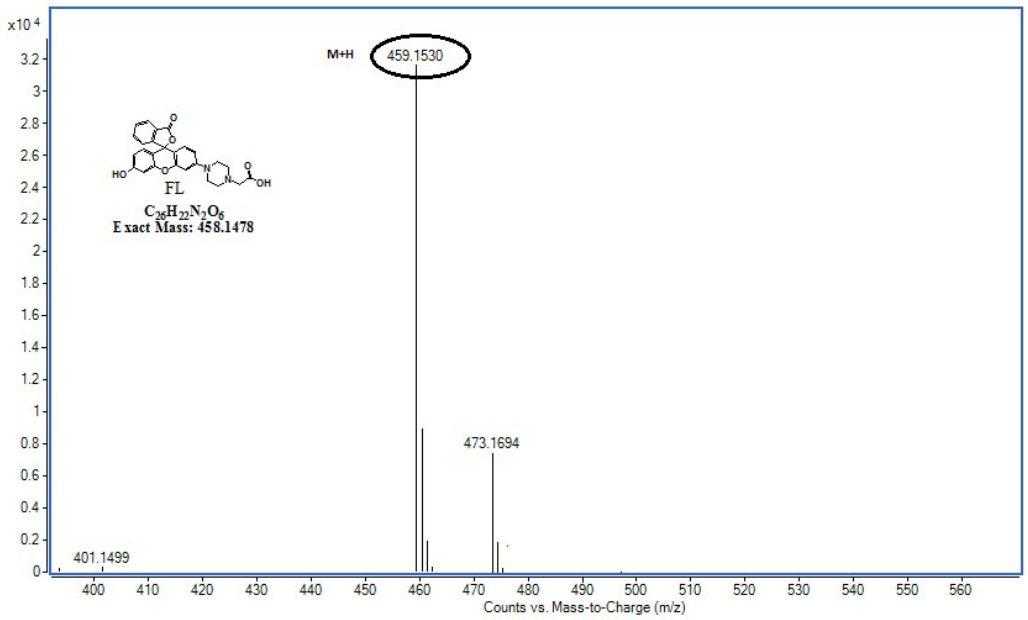


**Fig. S29. ESI-HRMS** of **ALP** treated **LP1.**

## *References*


[1] Gaussian 16, Revision A.03, M. J. Frisch, G. W. Trucks, H. B. Schlegel, G. E. Scuseria, M. A. Robb, J. R. Cheeseman, G. Scalmani, V. Barone, G. A. Petersson, H. Nakatsuji, X. Li, M. Caricato, A. V. Marenich, J. Bloino, B. G. Janesko, R. Gomperts, B. Mennucci, H. P. Hratchian, J. V. Ortiz, A. F. Izmaylov, J. L. Sonnenberg, D. Williams-Young, F. Ding, F. Lipparini, F. Egidi, J. Goings, B. Peng, A. Petrone, T. Henderson, D. Ranasinghe, V. G. Zakrzewski, J. Gao, N. Rega, G. Zheng, W. Liang, M. Hada, M. Ehara, K. Toyota, R. Fukuda, J. Hasegawa, M. Ishida, T. Nakajima, Y. Honda, O. Kitao, H. Nakai, T. Vreven, K. Throssell, J. A. Montgomery, Jr., J. E. Peralta, F. Ogliaro, M. J. Bearpark, J. J. Heyd, E. N. Brothers, K. N. Kudin, V. N. Staroverov, T. A. Keith, R. Kobayashi, J. Normand, K. Raghavachari, A. P. Rendell, J. C. Burant, S. S. Iyengar, J. Tomasi, M. Cossi, J. M. Millam, M. Klene, C. Adamo, R. Cammi, J. W. Ochterski, R. L. Martin, K. Morokuma, O. Farkas, J. B. Foresman, and D. J. Fox, Gaussian, Inc., Wallingford CT, 2016.

[2] W. Zhao, L. Baohui, X. Shuyong, Z. Qiang, *J. Theor. Comput. Chem.*, 2015, **14**, 13.

[3] R. G. Parr, R. A. Donnelly, M. Levy, W. E. Palke, *J. Chem. Phys.*, 1978, **68**, 3801.

[4] T. A. Koopmans, , *Physica*, 1993, **1**, 104-113.

[5] R. G. Parr, L. V. Szentpaly S. Liu, *J. Am. Chem. Soc*., 1999, **121**, 1922-1924.

[6] C. R. Calladine, H. R. Drew, B. F. Luisi, A. A. Travers, In Understanding DNA the Molecule and How it Works, 3rd ed., Elsevier, UK 2004, Ch. 11, pp. 270–294.

[7] C. Morell, A. Grand, A. Toro-Labbe, *J. Phys. Chem.* A , 2005, **109**, 205-212.